Explaining the $\mathcal{R}(D)$ and $\mathcal{R}(D^*)$ anomalies in the $B-L$ supersymmetric standard model with inverse seesaw mechanism

Dris Boubaa,[1,2] Shaaban Khalil,[3] Stefano Moretti,[4,5] and Cem Salih Un[6,7]

[1]*Laboratoire de Physique des Particules et Physique Statistique, Ecole Normale Supérieure-Kouba, B.P. 92, 16050, Vieux-Kouba, Algiers, Algeria*
[2]*Department of Matter sciences, Faculty of Science and Technology, Abbes Laghrour University Of Khenchela, B.P. 1252 Road of Batna, Khenchela 40004, Algeria*
[3]*Center for Fundamental Physics, Zewail City of Science and Technology, Sheikh Zayed,12588, Giza, Egypt*
[4]*School of Physics and Astronomy, University of Southampton, Highfield, Southampton SO17 1BJ, United Kingdom*
[5]*Department of Physics and Astronomy, Uppsala University, Box 516, SE-751 20 Uppsala, Sweden*
[6]*Department of Physics, Bursa Uludağ University, TR16059 Bursa, Turkey*
[7]*Departamento de Ciencias Integradas y Centro de Estudios Avanzados en Física Matemáticas y Computación, Campus del Carmen, Universidad de Huelva, Huelva 21071, Spain*

(Received 29 January 2023; accepted 3 April 2023; published 19 April 2023)

We investigate the $\mathcal{R}(D)$ and $\mathcal{R}(D^*)$ anomalies in the context of the $B-L$ extension of the minimal supersymmetric Standard Model with inverse seesaw. We demonstrate that the lepton penguin $W^{\pm}l\bar{\nu}_l$ ($l=e,\mu,\tau$) mediated by CP-even/odd right-handed sneutrinos, charginos, and neutralinos can account for these anomalies simultaneously.

DOI: 10.1103/PhysRevD.107.075024

I. INTRODUCTION

In the many successes of the Standard Model (SM), the B-mesons and their decays play an important role. In particular, in addition to the observation of $B_s \to X_s\gamma$ and $B_s \to \mu^+\mu^-$ [1,2] decays, the precise experimental measurements of their property provide an elegant way to determine the Cabibbo-Kobayashi-Maskawa (CKM) matrix elements [3]. Furthermore, these decays are quite sensitive to new physics (NP) contributions, especially those happening through the transitions $b\to cl\bar{\nu}_l$ ($l=e,\ \mu,\ \tau$). Despite this dynamics occurs at tree-level in the SM, NP contributions at the same order of even at the loop level can be significant [4–8]. Also, compared with other semileptonic decays of B-meson, the $B\to D^{(*)}X$ ones are more advantageous since they are not CKM suppressed and thus can be probed through many (differential) observables [9,10]. If Lepton Flavour Universality (LFU) is exact up to the lepton masses, the SM predicts the following branching ratios (BRs): $\mathrm{BR}(B\to D\tau\overline{\nu_\tau})\simeq 0.64\%$ and $\mathrm{BR}(B\to D^*\tau\overline{\nu_\tau})\simeq 1.29\%$ [11]. Table I collects the results from the LHCb, *BABAR*, and Belle collaborations reported between 2012 and 2020 in terms of the ratios

$$\mathcal{R}(D)=\frac{\mathrm{BR}(B\to D\tau\overline{\nu_\tau})}{\mathrm{BR}(B\to Dl\overline{\nu_l})},$$
$$\mathcal{R}(D^*)=\frac{\mathrm{BR}(B\to D^*\tau\overline{\nu_\tau})}{\mathrm{BR}(B\to D^*l\overline{\nu_l})}. \tag{1}$$

Herein, the last row provides the combined results obtained by the Heavy Flavour Averaging (HFLAV) group.

The deviations between the experimental measurements and the SM predictions may hint at violation of LFU, which necessitates NP contributions [5,7,21–37]. One of the most promising beyond the SM (BSM) theories is supersymmetry (SUSY). In the minimal supersymmetric SM (MSSM), its minimal version, one may assume nonzero mixing among the slepton families to induce LFU violation at loop level. However, such a direct mixing is strictly constrained (see, e.g., [38]) by lepton flavor violation (LFV) experiments [39,40]. Nonetheless, the MSSM can still accommodate some deviations in $\mathcal{R}(D)$ and $\mathcal{R}(D^*)$ through the penguin diagrams involving neutralinos, charginos, and heavy Higgs bosons, but their contributions cannot fully recover the experimental

TABLE I. Experimental values for $\mathcal{R}(D)$ and $\mathcal{R}(D^*)$ reported by the experimental collaborations and HFLAV group.

	$\mathcal{R}(D)$	$\mathcal{R}(D^*)$
SM	0.299 ± 0.003 [9]	0.258 ± 0.005 [9]
LHCb		$0.336\pm0.027\pm0.030$ [12]
		$0.283\pm0.019\pm0.029$ [13,14]
Belle	$0.375\pm0.064\pm0.026$ [15]	$0.283\pm0.018\pm0.014$ [15]
	$0.307\pm0.037\pm0.016$ [15]	$0.293\pm0.038\pm0.015$ [16]
		$0.270\pm0.035^{+0.028}_{-0.025}$ [17,18]
BABAR	$0.440\pm0.058\pm0.042$ [19,20]	$0.332\pm0.024\pm0.018$ [19,20]
HFLAV	$0.339\pm0.026\pm0.014$ [2]	$0.295\pm0.010\pm0.010$ [2]

measurements [41–43]. In this paper, we surpass the MSSM by assuming that SUSY is nonminimal [44].

II. THE SUSY MODEL

The $B-L$ extension of the MSSM with inverse seesaw (BLSSM-IS) is based on the gauge group $SU(3)_C \times SU(2)_L \times U(1)_Y \times U(1)_{B-L}$, where $U(1)_{B-L}$ is spontaneously broken by two chiral singlet superfields $\hat{\chi}_{1,2}$ with $B-L$ charge $= \pm 1$. In addition to the MSSM superfields, a gauge boson Z'_{B-L} and three chiral singlet superfields $\hat{\nu}_i^c$ with $B-L$ charge $= -1$ are introduced for the consistency of the model. Finally, three singlet fermions S_1 with $B-L$ charge $= -2$ and three singlet fermions S_2 with $B-L$ charge $= +2$ are employed to implement the IS mechanism [45]. The superpotential of this model is given by

$$W = Y_u \hat{Q}\hat{H}_2 U^c + Y_d \hat{Q}\hat{H}_1 \hat{D}^c + Y_e \hat{L}\hat{H}_1 \hat{E}^c + Y_\nu \hat{L}\hat{H}_2 \hat{\nu}^c + Y_S \hat{\nu}^c \hat{\chi}_1 \hat{S}_2 + \mu \hat{H}_1 \hat{H}_2 + \mu' \hat{\chi}_1 \hat{\chi}_2. \quad (2)$$

Electroweak symmetry breaking (EWSB) and $B-L$ radiative breaking at $v' = \sqrt{v_1'^2 + v_2'^2} \gtrsim 7$ TeV are described in [46]. Here, we only consider the particle spectrum (masses and couplings) relevant to our processes, i.e., the BLSSM-IS lightest right-handed sneutrino and neutralino, with the lightest chargino being MSSM-like. If we write $\tilde{\nu}_L, \tilde{\nu}_R$ and $\tilde{S}_2$ in terms of real and imaginary parts, one finds that the mass of the lightest CP-odd sneutrino, $\tilde{\nu}_1^I$, is almost equal to that of the lightest CP-even one, $\tilde{\nu}_1^R$, and either can be of $\mathcal{O}(100$ GeV) [47].

The neutralinos $\tilde{\chi}_i^0$ $(i = 1, \ldots, 7)$ in the BLSSM-IS are the physical (mass) superpositions of three fermionic partners of the neutral gauge bosons called gauginos $\tilde{B}$ (bino), $\tilde{W}^3$ (wino) and $\tilde{B}'$ (B'ino), in addition to the fermionic partners of both the MSSM Higgs bosons ($\tilde{H}_1^0$ and $\tilde{H}_2^0$) and $B-L$ (pseudo)scalar bosons ($\tilde{\chi}_1$ and $\tilde{\chi}_2$). The lightest neutralino has the following decomposition:

$$\tilde{\chi}_1^0 = V_{11}\tilde{B} + V_{12}\tilde{W}^3 + V_{13}\tilde{H}_1^0 + V_{14}\tilde{H}_2^0 + V_{15}\tilde{B}' + V_{16}\tilde{\chi}_1 + V_{17}\tilde{\chi}_2. \quad (3)$$

In addition to the typical MSSM gaugino or Higgsino, the lightest supersymmetric particle (LSP) might be B'ino-like or $\tilde{\chi}_i$-like of order $\mathcal{O}(100$ GeV). It is worth noting that a salient feature of the BLSSM-IS model is the large neutrino couplings, which significantly contribute to lepton nonuniversality. Furthermore, in this model, two right-handed sneutrinos (one from each of CP-even and CP-odd sneutrinos) could be light (of order few hundred GeV), thereby contributing to the enhancement at one-loop through the diagrams involving these sneutrinos.

III. CONTRIBUTIONS TO $\mathcal{R}(D)$ AND $\mathcal{R}(D^*)$

The effective Hamiltonian for $b \to c l \bar{\nu}_l$ is given by

$$\mathcal{H}_{\rm eff} = \frac{4G_F V_{cb}}{\sqrt{2}}[(1+g_{VL})[\bar{c}\gamma^\mu P_L b][\bar{l}\gamma_\mu P_L \nu_l] + g_{VR}[\bar{c}\gamma^\mu P_R b][\bar{l}\gamma_\mu P_L \nu_l] + g_{SL}[\bar{c}P_L b][\bar{l}P_L \nu_l] + g_{SR}[\bar{c}P_R b][\bar{l}P_L \nu_l] + g_T[\bar{c}\sigma^{\mu\nu}P_L b][\bar{l}\sigma_{\mu\nu}P_L \nu_l]], \quad (4)$$

where G_F is the Fermi constant, V_{cb} is the CKM term which encodes the $b \to c$ transition, g_i is a ratio of the Wilson coefficients defined as $g_i \equiv C_i^{\rm SUSY}/C_i^{\rm SM}$ with $i = VL, VR, SL, SR, T$ and $P_{L,R}$ are the projection operators. In our notation, V, S, T stand for vector, scalar and tensor while L, R is the helicity state of the b-quark.

The observables $\mathcal{R}(D)$ and $\mathcal{R}(D^*)$ can be defined as

$$\mathcal{R}(D) = \frac{\Gamma(\bar{B} \to D\tau\nu_\tau)}{\Gamma(\bar{B} \to Dl\nu_l)} = \frac{\int_{m_\tau^2}^{(m_B - m_D)^2} \frac{d\Gamma_\tau^D}{dq^2} dq^2}{\int_{m_l^2}^{(m_B - m_D)^2} \frac{d\Gamma_l^D}{dq^2} dq^2}, \quad (5)$$

$$\mathcal{R}(D^*) = \frac{\Gamma(\bar{B} \to D^*\tau\nu_\tau)}{\Gamma(\bar{B} \to D^*l\nu_l)} = \frac{\int_{m_\tau^2}^{(m_B - m_D^*)^2} \frac{d\Gamma_\tau^{D^*}}{dq^2} dq^2}{\int_{m_l^2}^{(m_B - m_D^*)^2} \frac{d\Gamma_l^{D^*}}{dq^2} dq^2}. \quad (6)$$

The explicit dependence of $\mathcal{R}(D)$ and $\mathcal{R}(D^*)$ on the NP Wilson coefficients can be extracted by integrating the expressions for the differential decay rates in Refs. [28,35], where the helicity suppression effect (squared light charged lepton mass ratio) is negligible, and fix the form factors to their central values as in Ref. [2]. Therefore, one finds

$$\mathcal{R}(D) = \frac{\Gamma_\tau^D}{\Gamma_e^D}, \qquad \mathcal{R}(D^*) = \frac{\Gamma_\tau^{D^*}}{\Gamma_e^{D^*}}, \quad (7)$$

where

$$\Gamma_\tau^D = 10^{-15}(2.632|g_{SR}^\tau + g_{SL}^\tau|^2 + 2.810|1 + g_{VL}^\tau + g_{VR}^\tau|^2 + 2.309|g_T^\tau|^2 + 4\,\mathrm{Re}[(1 + g_{VL}^\tau + g_{VR}^\tau)(g_{SR}^\tau + g_{SL}^\tau)^*] + 3.064\,\mathrm{Re}[(1 + g_{VL}^\tau + g_{VR}^\tau)g_T^{\tau^*}]), \tag{8}$$

$$\Gamma_e^D = 10^{-15}(10|g_{SR}^e + g_{SL}^e|^2 + 9.393|1 + g_{VL}^e + g_{VR}^e|^2 + 6.293|g_T^e|^2 + 6.755\times 10^{-3}\,\mathrm{Re}[(1 + g_{VL}^e + g_{VR}^e)(g_{SR}^e + g_{SL}^e)^*] + 8.559\times 10^{-3}\,\mathrm{Re}[(1 + g_{VL}^e + g_{VR}^e)g_T^{e^*}]), \tag{9}$$

$$\Gamma_\tau^{D^*} = 10^{-14}(1.264\times 10^{-2}|g_{SR}^\tau - g_{SL}^\tau|^2 + 0.511(|1 + g_{VL}^\tau|^2 + |g_{VR}^\tau|^2) + 8.570|g_T^\tau|^2 + 4.82\times 10^{-2}\,\mathrm{Re}[(1 + g_{VL}^\tau + g_{VR}^\tau) \times (g_{SR}^\tau - g_{SL}^\tau)^*] + 3.333\,\mathrm{Re}[g_{VR}^\tau g_T^{\tau*}] - 2.278\,\mathrm{Re}[(1 + g_{VL}^\tau)g_T^{\tau*}] - 0.907\,\mathrm{Re}[(1 + g_{VL}^\tau)g_{VR}^{\tau*}]), \tag{10}$$

$$\Gamma_e^{D^*} = 10^{-14}(7.566\times 10^{-2}|g_{SR}^e - g_{SL}^e|^2 + 2.033(|1 + g_{VL}^e|^2 + |g_{VR}^e|^2) + 34.807|g_T^e|^2 + 1.583\times 10^{-3}\,\mathrm{Re}[(1 + g_{VL}^e + g_{VR}^e)(g_{SR}^e - g_{SL}^e)^*] + 7.067\times 10^{-3}\,\mathrm{Re}[g_{VR}^e g_T^{e*}] - 3.516\times 10^{-3}\,\mathrm{Re}[(1 + g_{VL}^e)g_T^{\tau*}] - 3.514\,\mathrm{Re}[(1 + g_{VL}^e)g_{VR}^{e*}]), \tag{11}$$

where the above decay rates can be constrained by $\Gamma(W\to\tau\nu)/\Gamma(W\to l\nu)$ and $\Gamma(\tau\to\mu\nu_\tau\nu_\mu)/\Gamma(\tau\to e\nu_\tau\nu_e)$. To determine the SM prediction for $\mathcal{R}(D)$ and $\mathcal{R}(D^*)$ the NP Wilson coefficients are set to zero, $g_i = 0$.

The penguin corrections to the vertex $W^\pm l\nu_l$ $(l = e, \mu, \tau)$ yield the SUSY contributions to g_{VL}. These corrections are achieved in the MSSM by exchanging charginos, neutralinos, and sleptons or left-handed sneutrinos. In the BLSSM-IS, the right-handed sneutrino with large Y_ν coupling can boost these contributions, as shown in Fig. 1. The relevant Wilson coefficient is given by

$$C_{VL}^{\tilde{\nu}^{\mathrm{R}}} = \frac{\Gamma^L_{\tilde{\chi}_b^0 \nu_k \tilde{\nu}_a^R}\Gamma^R_{\overline{l_l}\tilde{\chi}_c^- \tilde{\nu}_a^R}\Gamma^L_{\overline{u_j} d_i W^-}}{16\pi^2 m_{W^-}^2}[-\Gamma^L_{\tilde{\chi}_c^-\tilde{\chi}_b^0 W^-} m_{\tilde{\chi}_b^0} m_{\tilde{\chi}_c^-} - C_0(m^2_{\tilde{\chi}_c^-}, m^2_{\tilde{\chi}_b^0}, m^2_{\tilde{\nu}_a^R}) + \Gamma^R_{\tilde{\chi}_c^-\tilde{\chi}_b^0 W^-}[B_0(m^2_{\tilde{\chi}_b^0}, m^2_{\tilde{\chi}_c^-}) - 2C_{00}(m^2_{\tilde{\chi}_c^-}, m^2_{\tilde{\chi}_b^0}, m^2_{\tilde{\nu}_a^R}) + m^2_{\tilde{\nu}_a^R} C_0(m^2_{\tilde{\chi}_c^-}, m^2_{\tilde{\chi}_b^0}, m^2_{\tilde{\nu}_a^R})]], \tag{12}$$

with $R\to I$ for the CP-odd right-handed sneutrino. Here, $C_0(x,y,z)$, $B_0(x,y)$ and $C_{00}(x,y,z)$ are the loop functions defined in [48] and Γ stands for the coupling among the particles stated in the subindex.

The W decay to $l\nu$, whose ratio is subject to the experimental constraints [49]

$$W_{\tau e} \equiv \frac{\Gamma(W\to\tau\nu)}{\Gamma(W\to e\nu)} = 1.043 \pm 0.024,$$
$$W_{\tau\mu} \equiv \frac{\Gamma(W\to\tau\nu)}{\Gamma(W\to\mu\nu)} = 1.07 \pm 0.026, \tag{13}$$

may be affected by the mentioned penguin corrections.

Along with the leptonic decays of W boson, the precise measurements on the τ decays also play an important role to control violations to LFU. The following constraints are taken into account from experimental findings [49]:

$$\tau_{\mu e} \equiv \frac{\Gamma(\tau\to\mu\nu_\tau\nu_\mu)}{\Gamma(\tau\to e\nu_\tau\nu_e)} = 0.979 \pm 0.004. \tag{14}$$

One can also consider the loop diagrams like the first one in Fig. 1 for the leptonic decays of $Z-$boson which can be obtained by replacing the neutralino with the chargino. Even though the topologies seem the same, the main difference in the case of $Z-$boson decays arises from the behavior of the loop functions. Since the two charginos in the loop will be of the same mass, the loop functions, B_0, C_0, and C_{00}, will result in zero. Thus the leptonic decays of $Z-$boson remains intact. Note that this discussion does not hold if the second chargino runs in the loop along with the first chargino or one considers the self-energy diagrams in Fig. 1, but the contributions from these processes are severely suppressed due to the heavy masses of the involved particles.

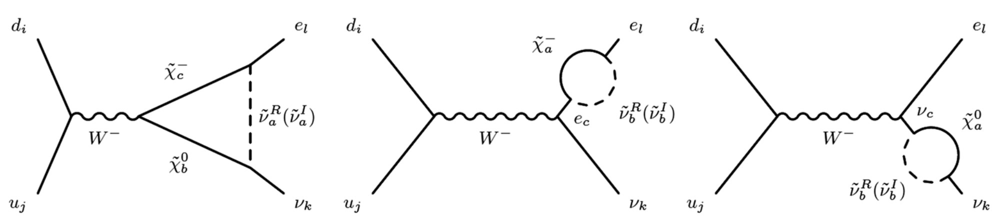

FIG. 1. Penguin and self-energy diagrams in the BLSSM-IS contributing to the $b\to\overline{c}l\bar{\nu}_l$ transition.

Furthermore, we apply the mass bounds on the SUSY spectrum [50–54], the constraints from the rare $B_s \to X_s\gamma$ and $B_s \to \mu^+\mu^-$ decay modes [2] as well as the current limits on the LFV processes as $l_i \to l_j\gamma$ [39,40].

IV. RESULTS

In this section, we display our results for $\mathcal{R}(D)$ and $\mathcal{R}(D^*)$ consistent with the experimental constraints mentioned above. We used the Metropolis-Hastings algorithm, as described in [55,56], combined with SPheno [57], in turn generated with SARAH [58], to scan the parameter space of the low scale BLSSM-IS. As some of the main contributions to $\mathcal{R}(D)$ and $\mathcal{R}(D^*)$ come through the first diagram in Fig. 1, involving the lightest chargino and neutralino, one would naively expect to observe the largest corrections for light masses of both of the latter. However, as shown in the left panel of Fig. 2, the experimental measurements of $\mathcal{R}(D)$ and $\mathcal{R}(D^*)$ can be accommodated within 2σ even when these particles weigh around 2 TeV (yellow points). Alas, the LFV and LFU constraints exclude these solutions and allow only those (red points) with $m_{\tilde{\chi}_1^\pm}, m_{\tilde{\chi}_1^0} \lesssim 1$ TeV.

The reason why even relatively heavy masses for the lightest chargino and neutralino can still accommodate the experimental measurements of $\mathcal{R}(D)$ and $\mathcal{R}(D^*)$ is due to the fact that one of the main drivers of the NP corrections is the mass degeneracy between these two states. As seen from the red points over the $m_{\tilde{\chi}_1^\pm} - m_{\tilde{\chi}_1^0}$ plane in the same plot, the enhancement in $\mathcal{R}(D)$ and $\mathcal{R}(D^*)$ mostly requires $m_{\tilde{\chi}_1^\pm} - m_{\tilde{\chi}_1^0} \simeq 0$. This degeneracy can be understood through the asymptotic behavior of the vector-like Wilson coefficient. When two of the particles in the triangle loops are nearly degenerate in mass, the NP contributions become proportional to the mass of the third particle in it, up to some scales at which the (phase space) suppression from the mass takes over [41,48]. Another fact leading to the mass degeneracy being instrumental to boost NP corrections is that the coupling $W - \tilde{\chi}^\pm - \tilde{\chi}^0$ takes its largest value when the chargino and neutralino are winolike and, indeed, the allowed SUSY spectra typically involve nearly mass degenerate winolike such states.

Considering the mass degeneracy and the asymptotic behavior of the loop functions in the Wilson coefficient given in Eq. (12), one can then expect that also heavy lightest right-handed sneutrino masses (essentially degenerate for CP-even and -odd states) can yield a considerable enhancement in $\mathcal{R}(D)$ and $\mathcal{R}(D^*)$. Indeed, the right panel of Fig. 2 shows that the $\mathcal{R}(D)$ and $\mathcal{R}(D^*)$ results in our model are almost insensitive to the (common) right-handed sneutrino mass, so that compliance with experimental measurements within 2σ can be realised when this state is as heavy as about 3.5 TeV.

Finally, we display the correlation between $\mathcal{R}(D)$ and $\mathcal{R}(D^*)$ in Fig. 3. Even though the theoretical solutions may not display any correlation (gray points), the experimental constraints allow only a linear relation between $\mathcal{R}(D)$ and $\mathcal{R}(D^*)$, i.e., $\mathcal{R}(D) \simeq 1.2 \times \mathcal{R}(D^*)$.

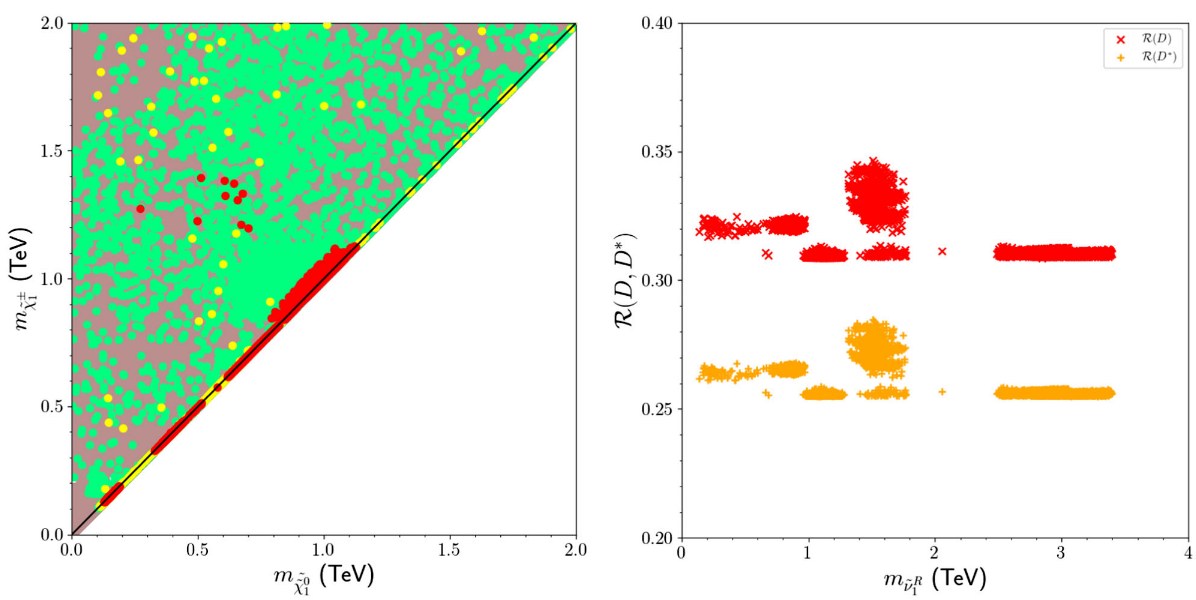

FIG. 2. $\mathcal{R}(D)$ and $\mathcal{R}(D^*)$ in correlation with the lightest chargino and neutralino (left) as well as right-handed sneutrino (right) masses. In the $m_{\tilde{\chi}_1^\pm} - m_{\tilde{\chi}_1^0}$ plane, all points are compatible with EWSB. Green points also satisfy the SUSY mass bounds and the constraints on $B_s \to \mu^+\mu^-$ and $B_s \to X_s\gamma$. Yellow points indicate the solutions for $\mathcal{R}(D)$ and $\mathcal{R}(D^*)$ within 2σ of the experimental measurements. The red points form a subset of the yellow ones as they are also consistent with LFV and LFU constraints. The correlation with the right-handed sneutrino mass (common to CP-even and -odd states) is shown only for these red points.

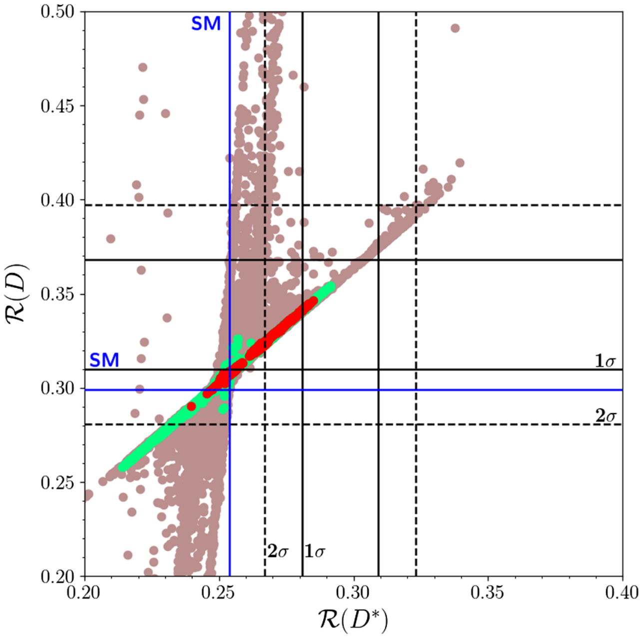

FIG. 3. The correlation between $\mathcal{R}(D)$ and $\mathcal{R}(D^*)$. Here, all points are compatible with EWSB. Green points also satisfy the SUSY mass bounds and the constraints from $B_s \to \mu^+\mu^-$ and $B_s \to X_s\gamma$. The red points form a subset of the green ones they are also consistent with LFV and LFU constraints. The horizontal (vertical) black solid and dashed lines show the 1σ and 2σ ranges of the experimental measurements of $\mathcal{R}(D)$ [$\mathcal{R}(D^*)$], respectively, while the blue line indicates the SM value.

V. CONCLUSIONS

We have found that the BLSSM-IS is able to explain within 1σ the (averaged) measured values of $\mathcal{R}(D)$ and $\mathcal{R}(D^*)$, in presence of experimental constraints on its EW, SUSY and flavor sectors, notably including those from LFU and LFV observables. The additional NP contributions, above and beyond the SM ones, that enable this are given by penguin diagrams involving the lightest CP-even/odd right-handed sneutrino, neutralino, and chargino. This result goes beyond what was previously achieved for the MSSM, which is only partially able to comply with the observed values of these quantities. Specifically, it is noteworthy that $\mathcal{R}(D)$ is enhanced in the BLSSM-IS significantly more than in the MSSM. This is due to the following two reasons. Firstly, the BLSSM-IS has additional right-handed sneutrinos (both real and imaginary components) running in the relevant penguin diagram with, owing to the IS dynamics for neutrino masses, large Yukawa couplings between a charged Higgsino, charged lepton and such a lightest right-handed sneutrino. Secondly, unlike in the MSSM, due to the significant contribution of such a right-handed sneutrino in the BLSSM-IS to both τ and light lepton ($\ell = e, \mu$) observables, Γ_ℓ can be suitably reduced with respect to its value in the SM. As overall result, the Γ_τ/Γ_ℓ ratio that defines $\mathcal{R}(D)$ is thus improved. In summary then, $\mathcal{R}(D)$ (especially) and $\mathcal{R}(D^*)$ (more moderately) appear to privilege a nonminimal realization of SUSY. Finally, in addition to its relevant contribution to both $\mathcal{R}(D)$ and $\mathcal{R}(D^*)$, the BLSSM-IS contains several signals that can be probed to confirm or refute this type of SM extension. For instance, the light right-handed sneutrino can be a viable scalar DM candidate with peculiar features. Also Z' and other non-MSSM spectrum can be examined at different processes at the LHC.

ACKNOWLEDGMENTS

D. B. is supported by the Algerian Ministry of Higher Education and Scientific Research under the PRFU Project No. B00L02UN400120230002. S. K. is partially supported by the Science, Technology and Innovation Funding Authority (STDF) under Grant No. 37272. S. M. is supported in part through the NExT Institute and the STFC Consolidated Grant No. ST/L000296/1. C. S. U. is supported in part by the Spanish MICINN, under Grant No. PID2019–107844GB-C22.

[1] LHCb Collaboration, First Evidence for the Decay $B_s^0 \to \mu^+\mu^-$, Phys. Rev. Lett. **110**, 021801 (2013).
[2] HFLAV Collaboration, Averages of b-hadron, c-hadron, and τ-lepton properties as of 2021, Phys. Rev. D **107**, 052008 (2023).
[3] LHCb Collaboration, First Observation of the Decay $B_s^0 \to K^-\mu^+\nu_\mu$ and Measurement of $|V_{ub}|/|V_{cb}|$, Phys. Rev. Lett. **126**, 081804 (2021).
[4] S. Fajfer, J. F. Kamenik, and I. Nisandzic, On the $B \to D^*\tau\bar{\nu}_\tau$ sensitivity to new physics, Phys. Rev. D **85**, 094025 (2012).
[5] A. Crivellin, C. Greub, and A. Kokulu, Explaining $B \to D\tau\nu$, $B \to D^*\tau\nu$ and $B \to \tau\nu$ in a 2HDM of type III, Phys. Rev. D **86**, 054014 (2012).
[6] A. Crivellin, A. Kokulu, and C. Greub, Flavor-phenomenology of two-Higgs-doublet models with generic Yukawa structure, Phys. Rev. D **87**, 094031 (2013).
[7] A. Celis, M. Jung, X.-Q. Li, and A. Pich, Sensitivity to charged scalars in $\boldsymbol{B \to D^{(*)}\tau\nu_\tau}$ and $\boldsymbol{B \to \tau\nu_\tau}$ decays, J. High Energy Phys. 01 (**2013**) 054.
[8] A. Celis, M. Jung, X.-Q. Li, and A. Pich, Scalar contributions to $b \to c(u)\tau\nu$ transitions, Phys. Lett. B **771**, 168 (2017).

[9] HFLAV Collaboration, Averages of b-hadron, c-hadron, and τ-lepton properties as of 2018, Eur. Phys. J. C **81**, 226 (2021).

[10] M. Duraisamy, P. Sharma, and A. Datta, Azimuthal $B \to D^* \tau^- \overline{\nu_\tau}$ angular distribution with tensor operators, Phys. Rev. D **90**, 074013 (2014).

[11] C.-H. Chen and C.-Q. Geng, Charged Higgs on $B \to \tau \bar{\nu}_\tau$ and $\bar{B} \to P(V) l \bar{\nu})_l$, J. High Energy Phys. 10 (2006) 053.

[12] LHCb Collaboration, Measurement of the Ratio of Branching Fractions $\mathcal{B}(\bar{B}^0 \to D^{*+} \tau^- \bar{\nu}_\tau)/\mathcal{B}(\bar{B}^0 \to D^{*+} \mu^- \bar{\nu}_\mu)$, Phys. Rev. Lett. **115**, 111803 (2015).

[13] LHCb Collaboration, Measurement of the Ratio of the $B^0 \to D^{*-} \tau^+ \nu_\tau$ and $B^0 \to D^{*-} \mu^+ \nu_\mu$ Branching Fractions Using Three-Prong τ-Lepton Decays, Phys. Rev. Lett. **120**, 171802 (2018).

[14] LHCb Collaboration, Test of Lepton Flavor Universality by the measurement of the $B^0 \to D^{*-} \tau^+ \nu_\tau$ branching fraction using three-prong τ decays, Phys. Rev. D **97**, 072013 (2018).

[15] Belle Collaboration, Measurement of $\mathcal{R}(D)$ and $\mathcal{R}(D^*)$ with a Semileptonic Tagging Method, Phys. Rev. Lett. **124**, 161803 (2020).

[16] Belle Collaboration, Measurement of the branching ratio of $\bar{B} \to D^{(*)} \tau^- \bar{\nu}_\tau$ relative to $\bar{B} \to D^{(*)} \ell^- \bar{\nu}_\ell$ decays with hadronic tagging at Belle, Phys. Rev. D **92**, 072014 (2015).

[17] Belle Collaboration, Measurement of the τ lepton polarization and $R(D^*)$ in the decay $\bar{B} \to D^* \tau^- \bar{\nu}_\tau$ with one-prong hadronic τ decays at Belle, Phys. Rev. D **97**, 012004 (2018).

[18] Belle Collaboration, Measurement of the τ Lepton Polarization and $R(D^*)$ in the Decay $\bar{B} \to D^* \tau^- \bar{\nu}_\tau$, Phys. Rev. Lett. **118**, 211801 (2017).

[19] *BABAR* Collaboration, Evidence for an Excess of $\bar{B} \to D^{(*)} \tau^- \bar{\nu}_\tau$ Decays, Phys. Rev. Lett. **109**, 101802 (2012).

[20] *BABAR* Collaboration, Measurement of an excess of $\bar{B} \to D^{(*)} \tau^- \bar{\nu}_\tau$ decays and implications for charged Higgs bosons, Phys. Rev. D **88**, 072012 (2013).

[21] A. Crivellin, D. Müller, and F. Saturnino, Flavor phenomenology of the leptoquark singlet-triplet model, J. High Energy Phys. 06 (2020) 020.

[22] J. D. Gómez, N. Quintero, and E. Rojas, Charged current $b \to c \tau \bar{\nu}_\tau$ anomalies in a general W' boson scenario, Phys. Rev. D **100**, 093003 (2019).

[23] C. Marzo, L. Marzola, and M. Raidal, Common explanation to the $R_{K^{(*)}}$, $R_{D^{(*)}}$ and ϵ'/ϵ anomalies in a 3HDM $+ \nu_R$ and connections to neutrino physics, Phys. Rev. D **100**, 055031 (2019).

[24] X.-G. He and G. Valencia, Lepton universality violation and right-handed currents in $b \to c \tau \nu$, Phys. Lett. B **779**, 52 (2018).

[25] S. Iguro and K. Tobe, $R(D^{(*)})$ in a general two Higgs doublet model, Nucl. Phys. **B925**, 560 (2017).

[26] M. Wei and Y. Chong-Xing, Charged Higgs bosons from the $3-3-1$ models and the $\mathcal{R}(D^{(*)})$ anomalies, Phys. Rev. D **95**, 035040 (2017).

[27] B. Bhattacharya, A. Datta, J.-P. Guévin, D. London, and R. Watanabe, Simultaneous explanation of the R_K and $R_{D^{(*)}}$ puzzles: A model analysis, J. High Energy Phys. 01 (2017) 015.

[28] Y. Sakaki, M. Tanaka, A. Tayduganov, and R. Watanabe, Testing leptoquark models in $\bar{B} \to D^{(*)} \tau \bar{\nu}$, Phys. Rev. D **88**, 094012 (2013).

[29] P. Ko, Y. Omura, and C. Yu, $B \to D^{(*)} \tau \nu$ and $B \to \tau \nu$ in chiral $U(1)'$ models with flavored multi Higgs doublets, J. High Energy Phys. 03 (**2013**) 151.

[30] B. Bhattacharya, A. Datta, S. Kamali, and D. London, A measurable angular distribution for $\bar{B} \to D^* \tau^- \bar{\nu}_\tau$ decays, J. High Energy Phys. 07 (**2020**) 194.

[31] A. Datta, S. Kamali, S. Meinel, and A. Rashed, Phenomenology of $\Lambda_b \to \Lambda_c \tau \bar{\nu}_\tau$ using lattice QCD calculations, J. High Energy Phys. 08 (**2017**) 131.

[32] B. Bhattacharya, A. Datta, D. London, and S. Shivashankara, Simultaneous explanation of the R_K and $R(D^{(*)})$ puzzles, Phys. Lett. B **742**, 370 (2015).

[33] A. Datta, M. Duraisamy, and D. Ghosh, Diagnosing new physics in $b \to c \tau \nu_\tau$ decays in the light of the recent *BABAR* result, Phys. Rev. D **86**, 034027 (2012).

[34] S. Fajfer, J. F. Kamenik, I. Nisandzic, and J. Zupan, Implications of Lepton Flavor Universality Violations in B Decays, Phys. Rev. Lett. **109**, 161801 (2012).

[35] M. Tanaka and R. Watanabe, New physics in the weak interaction of $\bar{B} \to D^{(*)} \tau \bar{\nu}$, Phys. Rev. D **87**, 034028 (2013).

[36] A. K. Alok, D. Kumar, J. Kumar, S. Kumbhakar, and S. U. Sankar, New physics solutions for R_D and R_{D^*}, J. High Energy Phys. 09 (2018) 152.

[37] A. K. Alok, D. Kumar, S. Kumbhakar, and S. Uma Sankar, Solutions to $R_D - R_{D^*}$ in light of Belle 2019 data, Nucl. Phys. **B953**, 114957 (2020).

[38] A. Hammad, S. Khalil, and C. S. Un, Large BR($h \to \tau \mu$) in supersymmetric models, Phys. Rev. D **95**, 055028 (2017).

[39] MEG II Collaboration, The search for $\mu^+ \to e^+ \gamma$ with 10–14 Sensitivity: The upgrade of the MEG experiment, Symmetry **13**, 1591 (2021).

[40] *BABAR* Collaboration, Searches for Lepton Flavor Violation in the Decays $\tau^{+-} \to e^{+-} \gamma$ and $\tau^{+-} \to mu^{+-} \gamma$, Phys. Rev. Lett. **104**, 021802 (2010).

[41] D. Boubaa, S. Khalil, and S. Moretti, Alleviating the $\bar{B} \to D \tau \nu$ and $\bar{B} \to D^* \tau \nu_\tau$ puzzle in the MSSM, Int. J. Mod. Phys. A **34**, 1950209 (2019).

[42] D. Boubaa, S. Khalil, and S. Moretti, Explaining B decays anomalies in SUSY models, J. Phys. Conf. Ser. **1766**, 012018 (2021).

[43] Q.-Y. Hu, Y.-D. Yang, and M.-D. Zheng, Revisiting the B-physics anomalies in R-parity violating MSSM, Eur. Phys. J. C **80**, 365 (2020).

[44] S. Moretti and S. Khalil, *Supersymmetry Beyond Minimality: From Theory to Experiment* (CRC Press, 2019).

[45] S. Khalil, TeV-scale gauged B-L symmetry with inverse seesaw mechanism, Phys. Rev. D **82**, 077702 (2010).

[46] S. Khalil, Radiative symmetry breaking in supersymmetric $B-L$ models with an inverse seesaw mechanism, Phys. Rev. D **94**, 075003 (2016).

[47] S. Khalil and S. Moretti, The $B-L$ supersymmetric standard model with inverse seesaw at the large hadron collider, Rep. Prog. Phys. **80**, 036201 (2017).

[48] A. J. Buras, P. H. Chankowski, J. Rosiek, and L. Slawianowska, $\Delta M_{d,s}, B^0 d, s \to \mu^+ \mu^-$ and $B \to X_s \gamma$ in supersymmetry at large $\tan\beta$, Nucl. Phys. **B659**, 3 (2003).

[49] Particle Data Group, Review of particle physics, Chin. Phys. C **40**, 100001 (2016).

[50] Particle Data Group, Review of particle physics, Chin. Phys. C **38**, 090001 (2014).
[51] ATLAS Collaboration, Observation of a new particle in the search for the Standard Model Higgs boson with the ATLAS detector at the LHC, Phys. Lett. B **716**, 1 (2012).
[52] CMS Collaboration, Observation of a new boson at a mass of 125 GeV with the CMS Experiment at the LHC, Phys. Lett. B **716**, 30 (2012).
[53] ATLAS Collaboration, Search for squarks and gluinos in final states with jets and missing transverse momentum using 36 fb^{-1} of $\sqrt{s} = 13$ TeV pp collision data with the ATLAS detector, Phys. Rev. D **97**, 112001 (2018).
[54] ATLAS Collaboration, Search for heavy particles decaying into a top-quark pair in the fully hadronic final state in pp collisions at $\sqrt{s} = 13$ TeV with the ATLAS detector, Phys. Rev. D **99**, 092004 (2019).
[55] H. Baer, S. Kraml, S. Sekmen, and H. Summy, Dark matter allowed scenarios for Yukawa-unified SO(10) SUSY GUTs, J. High Energy Phys. 03 (2008) 056.
[56] G. Belanger, F. Boudjema, A. Pukhov, and R. K. Singh, Constraining the MSSM with universal gaugino masses and implication for searches at the LHC, J. High Energy Phys. 11 (2009) 026.
[57] W. Porod and F. Staub, SPheno 3.1: Extensions including flavour, *CP*-phases and models beyond the MSSM, Comput. Phys. Commun. **183**, 2458 (2012).
[58] F. Staub, SARAH 4: A tool for (not only SUSY) model builders, Comput. Phys. Commun. **185**, 1773 (2014).